European Journal of Nuclear Medicine and Molecular Imaging (2021) 48:1976–1986
https://doi.org/10.1007/s00259-020-05113-1

ORIGINAL ARTICLE

PET/MRI assessment of lung nodules in primary abdominal malignancies: sensitivity and outcome analysis

Pierpaolo Biondetti[1] · Mark G. Vangel[2] · Rita M. Lahoud[1] · Felipe S. Furtado[1] · Bruce R. Rosen[1,3] · David Groshar[4,5] · Lina G. Canamaque[6] · Lale Umutlu[7] · Eric W. Zhang[1] · Umar Mahmood[1,3] · Subba R. Digumarthy[1] · Jo-Anne O. Shepard[1] · Onofrio A. Catalano[1,3]

Received: 3 September 2020 / Accepted: 8 November 2020 / Published online: 7 January 2021

Abstract

Purpose To evaluate PET/MR lung nodule detection compared to PET/CT or CT, to determine growth of nodules missed by PET/MR, and to investigate the impact of missed nodules on clinical management in primary abdominal malignancies.

Methods This retrospective IRB-approved study included [18F]-FDG PET/MR in 126 patients. All had standard of care chest imaging (SCI) with diagnostic chest CT or PET/CT within 6 weeks of PET/MR that served as standard of reference. Two radiologists assessed lung nodules (size, location, consistency, position, and [18F]-FDG avidity) on SCI and PET/MR. A side-by-side analysis of nodules on SCI and PET/MR was performed. The nodules missed on PET/MR were assessed on follow-up SCI to ascertain their growth (≥ 2 mm); their impact on management was also investigated.

Results A total of 505 nodules (mean 4 mm, range 1–23 mm) were detected by SCI in 89/126 patients (66M:60F, mean age 60 years). PET/MR detected 61 nodules for a sensitivity of 28.1% for patient and 12.1% for nodule, with higher sensitivity for > 7 mm nodules (< 30% and > 70% respectively, $p < 0.05$). 75/337 (22.3%) of the nodules missed on PET/MR (follow-up mean 736 days) demonstrated growth. In patients positive for nodules at SCI and negative at PET/MR, missed nodules did not influence patients' management.

This article is part of the Topical Collection on Oncology - Chest

Key points

- Overall PET/MR demonstrated a sensitivity of 12.1% (95% CI 9.4% to 15.2%) and a specificity of 69.8% (95% CI 55.7% to 81.7%).
- PET/MR detection of nodules was influenced by size (< 15% for ≤ 5 mm, > 70% for > 7 mm, p=0.001) and unaffected by other factors such as lobar location and density. The mean size of the nodules missed on PET/MR was 3.6 mm.
- 22.3% (75/337) of the nodules missed by PET/MR grew by ≥ 2 mm. However, upon review, the detection of these nodules would not have influenced management in any patient as they already had established stage IV disease, or the presence of small lung nodules would not have affected debulking or definitive surgery.

✉ Onofrio A. Catalano
ocatalano@mgh.harvard.edu

[1] Department of Radiology, Massachusetts General Hospital, Harvard Medical School, 55 Fruit Street, White 270, Boston, MA 02114, USA

[2] Biostatistics Center, Massachusetts General Hospital, Harvard Medical School, 60 Staniford St, Boston, MA, USA

[3] Athinoula A Martinos Center for Biomedical Imaging, Department of Radiology, Massachusetts General Hospital and Harvard Medical School, Boston, MA, USA

[4] Department of Nuclear Medicine, Assuta Medical Centers, Tel Aviv, Israel

[5] Sackler School of Medicine, Tel Aviv University, Tel Aviv, Israel

[6] Department of Nuclear Medicine. Grupo HM Hospitales, Madrid, Spain

[7] Department of Diagnostic and Interventional Radiology and Neuroradiology, University Hospital Essen, Essen, Germany

Conclusions Sensitivity of lung nodule detection on PET/MR is affected by nodule size and is lower than SCI. 22.3% of missed nodules increased on follow-up likely representing metastases. Although this did not impact clinical management in study group with primary abdominal malignancy, largely composed of extra-thoracic advanced stage cancers, with possible different implications in patients without extra-thoracic spread.

Keywords PET/MRI · PET/MR · PET/CT · Lung nodule · Pulmonary nodule

Abbreviations and acronyms

[18F]-FDG	2-deoxy-2-[18F]fluoro-D-glucose
HASTE	T2-weighted half-Fourier single-shot turbo spine-echo
LAVA	Liver accelerated volume acquisition
SCI	Standard of care chest imaging
UTE	Ultrashort echo time sequence
VIBE	Volume-interpolated breath-hold examination
WB	Whole-body
BP	Bed position

Introduction

Pulmonary nodules are routinely detected in chest computed tomography (CT), with an incidence of 30% for nodules ≥ 4 mm [1]. Most commonly, lung nodules are benign and related to granulomatous disease, intrapulmonary lymph-nodes, prior infection, and infarction. The possibility of metastases should always be considered during oncologic work-up [2].

Currently, 2-deoxy-2-[18F]fluoro-D-glucose ([18F]-FDG) positron emission tomography/computed tomography (PET/CT) is considered the most accurate imaging technique for diagnosis, staging, and restaging several cancers. CT provides the anatomic map to co-register PET, allowing fusion of anatomical images with metabolic activity. Chest CT has high sensitivity for detecting lung nodules due to high contrast between the low density air-containing lung and the high density of lung nodules, with detection rates up to 30–97% [3]. Therefore, CT enables detection of lesions that can be missed by stand-alone PET, particularly for non-[18F]-FDG -avid cancers, due to low cellularity or metabolic activity such as, for example well-differentiated hepatocellular carcinoma. On the other hand, the picomolar sensitivity of PET aids in detecting metabolically avid lesions that can be missed on CT. PET/CT, by combining the advantages of both modalities, can outperform stand-alone PET and CT (sensitivity 82–95%, specificity 81–82% for malignant nodules) [4, 5], and is the technology of choice in evaluating pulmonary nodules > 1 cm [6–8].

Positron emission tomography/magnetic resonance imaging (PET/MR) is a hybrid imaging modality that simultaneously acquires PET and MR, integrating anatomical and functional data of MR with metabolic information and high sensitivity of PET. While PET/MR is shown to outperform PET/CT in the oncologic evaluation of the abdomen, pelvis, and bones, it underperforms for assessing lung nodules [9–15], which is a major factor for omitting PET/MR in oncologic staging. The reasons behind its lower sensitivity are low proton density in the air-filled lungs, fast signal decay, and cardiac and respiratory motion artifacts [16, 17]. The reported sensitivity of PET/MR in detecting lung nodules is lower than PET/CT (30–83% on a nodule basis) [18–24]. The MR sequences used in PET/MR included 3-dimensional (3D) ultrashort echo time sequence (UTE), T1-weighted 3D gradient echo, for example, volume-interpolated breath-hold examination (VIBE) or liver accelerated volume acquisition (LAVA), T2-weighted half-Fourier single-shot turbo spine-echo (HASTE), and diffusion-weighted imaging (DWI).

Nonetheless, the true impact of PET/MR in evaluating lung nodules is still unclear. Prior studies were limited by a small number of patients or nodules. Moreover, some studies set an arbitrary cut-off for the maximum number of nodules per patient or excluded upfront the assessment of smaller nodules below a set threshold. Others used the lower quality attenuation correction CT as reference standard, which is widely considered a non-diagnostic study. More importantly, little is known with regard to the significance and clinical outcome of nodules missed on PET/MR but detected on PET/CT [19, 23, 25].

The purpose of our study was to evaluate lung nodules on PET/MR compared to diagnostic CT and PET/CT as reference standard, to assess longitudinal evolution of missed nodules over time, and to determine the impact of missed nodules on clinical management in patients with primary abdominal malignancies.

Materials and methods

This retrospective cohort study was approved by the local ethical review board (Partners Healthcare IRB number 2018P001334) and carried out according to Good Clinical Practice Guidelines of the International Council on Harmonization and the Declaration of Helsinki. Institutional review boards waived requirement for patient consent.

Patient selection

The study period was between February 2017 and June 2018. Inclusion criteria were (1) primary abdominal malignancy, (2)

whole-body (WB) [18F]-FDG PET/MR including the chest, and (3) standard of care chest imaging (SCI) within 6 weeks from PET/MR with dedicated chest CT or WB [18F]-FDG PET/CT that included a diagnostic quality chest CT. Exclusion criteria were (1) severe artifacts limiting lung assessment, (2) moderate-to-large pleural effusion, causing relaxation atelectasis and potentially biasing the comparison, and (3) deviations from the standard scanning protocol specified below. A total of 131 consecutive patients were identified, but 5 were excluded due to concurrent primary lung cancer in 3, large pleural effusion in 1, and severe technical artifacts in 1 (study flow chart in Fig. 1).

SCI: CT and PET/CT protocols

We defined as SCI either stand-alone diagnostic chest CT or WB-PET/CT that always included diagnostic quality chest CT.

CTs were performed on various multidetector-row CT models from multiple vendors, with IV contrast injection, in inspiratory breath-hold, at 100–120 kV, and with automatic exposure control. The multiplanar chest CT images were reconstructed at 2.5- to 3-mm slice thickness using standard kernel. Lungs were evaluated in standard lung window setting.

All PET/CT was acquired on a Siemens Biograph PET/CT scanner (Siemens-Healthnieers, Erlangen, Germany) after standard protocol patient preparation, including 6-h fasting before scanning and confirming peripheral blood glucose < 200 mg/dL. An hour after injecting 555–925 MBq of [18F]-FDG (depending on weight), WB emission PET images were acquired from skull base to mid-thighs, with 6–8 bed positions (BP), 3 to 5 min/bed position. Attenuation correction was estimated on the non-contrast-enhanced CT: 120-keV, 11–100-mAs (based on BMI), 5-mm collimation, and 0.75 pitch. Diagnostic quality CT was acquired in all PET/CT in inspiration; slice/detector 64 × 0,6; pitch/speed 1,1; kv 120; mAs 150-230; acquisition slice thickness 3 mm, reconstruction slice thickness 1 mm; DFOV skin-to-skin; SFOV 500 mm.

PET data were reconstructed using OSEM algorithm with 2 or 3 iterations (BMI < 31 or ≥ 31 respectively), 8 subsets, and 5-mm Gaussian filter. Reconstructed images were evaluated in transverse, sagittal, and coronal planes, using Siemens TrueD workstation (Syngo TrueD; Siemens-Healthnieers, Erlangen, Germany).

PET/MR protocol

PET/MR images were obtained from skull base to mid-thighs, on a Biograph mMR scanner (Siemens-Healthnieers, Erlangen, Germany) using 5–6 BP depending on patient's height. PET/MR studies were performed either after a diagnostic PET/CT or independently. When independent, the radiotracer dose and technique were similar to PET/CT. Otherwise, PET/MR was acquired within 1 hour from PET/CT, with no additional [18F]-FDG injected. Chest MR sequences included inspiratory breath-hold post-contrast axial and coronal T1w VIBE and axial T2w HASTE, as in Table 1.

Lung nodule assessment

All images were evaluated in consensus, on a picture archiving and communication system workstation (PACS-AGFA Impax; AGFA Technical Imaging Systems, Ridgefield Park, NJ, USA), by a radiologist with 4 years of experience in chest imaging and a PET/MR expert with 8 years of experience. Readers were aware of the oncologic history but blinded to the diagnostic CT reports. SCI and PET/MR were separately and randomly interpreted in two separate sessions, at least 4 weeks apart to reduce recall bias.

PET-CT/CT

The lungs were evaluated in all planes to record non-calcified nodules of every size for each patient. Size was determined by longest diameter in millimeter. Lobar location, attenuation

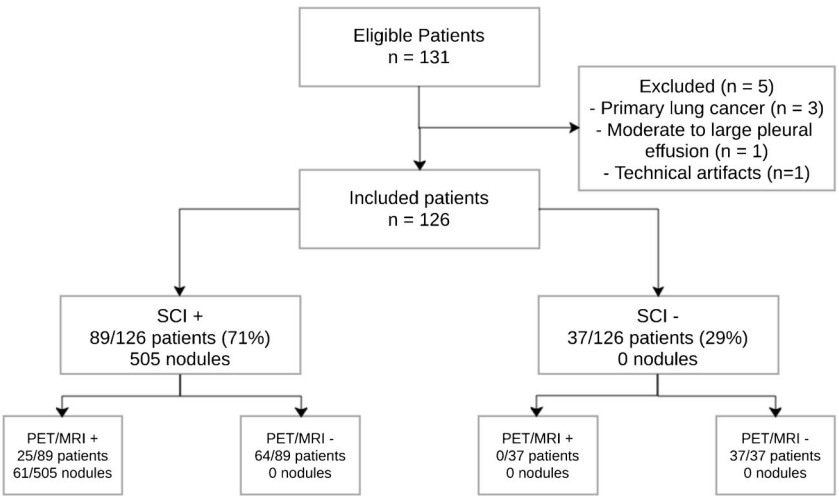

Fig. 1 Flowchart of population and design of this study

Table 1 PET/MRI protocol

	Sequence	Plane	iPat	Repetition Time (msec)	Echo Time (msec)	Inversion Time (msec)	Matrix	No. of Signals Acquired	Field of View (mm)	Section Thickness (mm)	Section Gap (mm)	Flip Angle (degrees)	Voxel Size (mm)	Fat Saturation
MR	T1w VIBE	Axial and coronal	2	4.06–4.1	1.81–1.91	NA	180 × 230	1	380	3.0	0	9	1.6 × 1.2 × 3.0	Quick spectral fat saturation
MR	T2w HASTE	Axial	2	1400	86–97	NA	288 × 384	1	380	6.0	0.6	NA	1.3 × 1.0 × 6.0	NA
PET	Acquisition time per BP (min)	Iterative reconstruction algorithm	Number subsets	Number iterations	Image grid	Voxel size (mm^3)	Axial field of view (mm)							
	4	3D attenuation weighted ordered subsets expectation maximization4	21	3	172 × 172	2.0 × 2.0 × 2.0	258							

BP, bed position; *HASTE*, T2-weighted half-Fourier single-shot turbo spine-echo; *iPAT*, integrated parallel acquisition techniques; *NA*, not applicable; *PET/MRI*, positron emission tomography/magnetic resonance imaging; *SE*, standard error; *CE-VIBE*, contrast-enhanced volume-interpolated breath-hold examination

(solid, partially solid, or ground-glass per glossary by Fleischner Society) [26], peripheral distribution (peripheral when ≤ 5 mm from parietal pleura, non-peripheral > 5 mm), and proximity to fissures (intra-fissural when in contact with the fissure and perifissural if within 5 mm) were also recorded. [18F]-FDG avidity was determined qualitatively by comparing to background lung activity. Nodule annotations were saved in PACS.

PET/MR

The above features were assessed also in PET/MR on axial and coronal T1w post-contrast VIBE and axial T2w HASTE images and annotations were saved in PACS. [18F]-FDG avidity was also recorded, with same criteria as for PET/CT, before and after fusion.

CT vs MR lung nodule comparison

The annotated nodules from diagnostic quality SCI CT, either obtained during PET/CT or stand-alone CT, were regarded as reference standard. The annotated nodules on PET/MR were compared side-by-side with the annotated SCI. A nodule was considered to be seen and true positive on PET/MR if it was noted in any sequence. Nodules that were not detected in any sequence were considered "missed" and false negative. Nodules noted only on PET/MR without CT correlates were considered false positives. Determination of true positives and false negatives was done on both individual patient and nodule basis. On patient basis, assessment was either positive, if ≥ 1 nodule was detected, or negative, if no nodule was detected.

Determining the significance of missed nodules on PET/MR

A nodule that increased ≥ 2 mm was defined "significant." The 2 mm threshold was chosen because in current Fleischer Society guidelines, it is considered a reasonable criterion for reporting growth of nodules. In fact, diameter measurements vary by 1.7 mm across observers for nodules smaller than 2 cm, so 2 mm would reduce likelihood of incorrect assessment of growth. Furthermore, several recent studies have used this 2-mm threshold to define growth in both solid and subsolid nodules. This threshold has also been adopted by the British Thoracic Society [26–31].

This determination of change in size was made on SCI. Electronic medical records were reviewed to determine if the nodule that was significant and missed on PET/MR would have impacted management. For instance, if a documented increase in a nodule in SCI was disregarded for clinical decisions, that nodule was deemed not to have influenced management. For this purpose, we also reported the tumor stage

before PET/MR acquisition, according to the 8th edition of the American Joint Committee on Cancer.

Statistical analysis

Categorical data are presented in number of occurrences with associated percentages. Continuous data are presented as median with interquartile ranges. Between-group comparisons for continuous data were performed using two-sample *t* test while between-group comparisons for categorical data were performed using Fisher's exact test. Pair-wise comparison between categorical data was performed using McNemar's test. Statistical significance was set at $p < 0.05$. All statistical analysis was performed using STATA 16 (StataCorp LLC, TX, USA).

Results

Patient and nodule characteristics

After exclusion of 5 patients, the study included 126 patients, mean age 59 years (± 12 SD), similar male/female distribution (Table 2). SCI was stand-alone chest CT in 53/126 (42.1%) and diagnostic-quality CT from PET/CT in 73/126 (57.9%). There were no lung nodules in 37 patients and 505 nodules in 89 patients on SCI. Table 3 details nodule characteristics.

PET/MR vs SCI

Overall sensitivity of PET/MR for lung nodules was 12.1% (61/505) (95% CI 9.4 to 15.2%), specificity 69.8% (95% CI 55.7 to 81.7%). There were 16 false-positive nodules on PET/MR. The detection of nodules on PET/MR was influenced by size (< 15% for ≤ 5 mm, > 70% for > 7 mm, $p = 0.001$) and unaffected by other factors such as lobar location and density. All perifissural and almost all fissural nodules were missed on PET/MR (Tables 4). Mean size of missed nodule was 3.6 mm. Per patient sensitivity of PET/MR was 28.1% (25/89) (Table 5). At least 1 nodule was detected in both SCI and PET/MR in 19.8% (25/126) of patients and no nodule in either modality in 29.4% (37/126). There was discordance in 50.8% (64/126) of patients where none of the nodules found on SCI was detected by PET/MR. PET/MR plot sensitivity values based on size are in Fig. 2, details in Table 6.

Table 2 Patient demographics and histology of primary cancers

Characteristics	All ($n = 126$)	Stage*
Age[a]		
Total	59 (±12; 24–82)	
Gender		
Male	66 (52.4%)	
Female	60 (47.6%)	
M:F ratio	1.1	
Malignancy subtypes		
Rectal adenocarcinoma	36 (28.6%)	I (5), III (11), IV (20)
Colon adenocarcinoma	27 (21.4%)	II (4), III (3), IV (20)
Cholangiocarcinoma	16 (12.7%)	I (1), II (2), III (3), IV (10)
Pancreatic ductal adenocarcinoma	15 (11.9%)	II (2), III (2), IV (11)
Anal squamous carcinoma	4 (3.2%)	III (2), IV (2)
Gallbladder adenocarcinoma	4 (3.2%)	II (1), III (1), IV (2)
Hepatocellular carcinoma	3 (2.4%)	II (1), III (1), IV (1)
Pancreatic neuroendocrine tumor	3 (2.4%)	III (1), IV (2)
Duodenal adenocarcinoma	2 (1.6%)	IV (2)
Esophageal adenocarcinoma	2 (1.6%)	III (1), IV (1)
Appendiceal adenocarcinoma	2 (1.6%)	IV (2)
Ovarian serous carcinoma	2 (1.6%)	IV (2)
Other malignancies	10 (7.8%)	III (3), IV (7)

n, number

[a] Values presented as mean (standard deviation; range). Otherwise, values are presented as number (percentage)

*Stage according to AJCC 8th edition has been reported in roman numbers; number of cases per each stage in parentheses

VIBE and HASTE vs SCI

Nodule detection between VIBE and HASTE was compared in 123 patients (3 patients excluded due to significant artifacts in VIBE) with 477 nodules seen on SCI. Both HASTE and VIBE detected 25 nodules, 11 nodules were seen exclusively on HASTE and 13 exclusively on VIBE (Fig. 3). Nodule detection was not significantly different between the two sequences, but sensitivity increased when the sequences were combined. Nodule detection sensitivity for HASTE and VIBE was 9.5% (48/505) and 8.0% (38/477) respectively. Per patient, sensitivity was 22.5% (20/89) for HASTE and 23.3% (20/86) for VIBE (Table 5). HASTE and VIBE plot sensitivity values based on size are displayed in Fig. 2.

^{18}F-FDG avidity: PET/MR vs PET/CT

Both PET/MR and PET/CT were performed in 57.9% (73/126). Nine nodules were [18F]-FDG avid in PET/CT and 10 in PET/MR (Fig. 4). Of these, 8 nodules were [18F]-FDG avid on both PET/CT and PET/MR and concordant. One nodule was [18F]-FDG avid only on PET/CT and 2 nodules only on PET/MR. Since PET/CT was considered reference standard, the nodules with and without [18F]-FDG avidity only on PET/MR were considered false positive and false negatives respectively.

Table 3 TILE: pulmonary nodule characteristics on SCI

Characteristics	SCI ($n = 505$)
Patients with nodules	89/126 (71%)
Nodules per patients	5.7 (1–27)
Size (mm)[a]	4 (± 2.5; 1–23)
Density	
Solid	483 (95.6%)
Ground glass	21 (4.2%)
Mixed attenuation	1 (0.2%)
Axial location	
Peripheral	374 (74%)
Non-peripheral	131 (26%)
Fissural relationship	
Intraparenchymal	460 (91%)
Intrafissural	35 (7%)
Perifissural	10 (2%)
Lobar location	
Right upper lobe	157 (31%)
Right middle lobe	60 (12%)
Right lower lobe	84 (17%)
Left upper lobe	104 (21%)
Left lower lobe	100 (20%)
Observation time[a,b] (days)	736 (± 466; 366–3004)

[a] Values presented as mean (standard deviation; range), otherwise, as number (percentage)

[b] observation time included a period of at least 12 months encompassing prior and/or follow-up imaging

Outcome of nodules missed on PET/MR and impact on management

A total of 337 nodules in 64 patients (64/126, 50.8%) were noted on SCI but not on PET/MR and constituted "missed" nodules. There was a size increase by ≥ 2 mm in 22.3% (75/337) nodules. However, upon review, the detection of these nodules would not have influenced management as patients in our cohort already had established advanced disease (stage III in 28 cases and stage IV in 80 cases), or occurrence of small lung nodules would not have affected debulking or definitive surgery (stages I and II in 16 cases, and stage IV in 2 cases of ovarian cancer). Please find the detailed cancer stages in Table 2.

Discussion

This is the largest study to date to compare lung nodule detection on PET/MR versus standard of care imaging CT. This is also the first study to include all nodules without adopting

Table 4 Impact of pulmonary nodule characteristics on PET/MRI detection

Characteristics	PET/MR $n = 61$	p value
Size (mm)[b]		
≤ 5 mm	32 (52%)	< 0.001
6–7 mm	12 (20%)	
> 7 mm	17 (28%)	
Density		
Solid	56 (92%)	0.08
Ground glass	4 (6%)	
Mixed attenuation	1 (2%)	
Location		
Peripheral	49 (80%)	0.46
Intermediate	10 (17%)	
Central	2 (3%)	
Fissural relationship		
Intraparenchymal	60 (99%)	0.10
Intrafissural	1 (1%)	
Perifissural	0 (0%)	
Lobar location		
Upper lobes	321	0.22
Lower lobes	184	

[a] Values presented as sensitivity. Otherwise, values are presented as number (percentage) with p values derived from Fisher's exact test

Table 5 Comparison between SCI and PET/MR including VIBE and HASTE for pulmonary nodule detection in 89/126 patients who were positive for lung nodules

Characteristics	SCI (standard reference)	PET/MRI	*p* value[#]	VIBE[a]	HASTE[a]	*p* value*
Nodule						
Yes	505 (100%)	61 (12%)	< 0.00001	38 (8%)	36 (8%)	0.84
No	0 (0%)	444 (88%)		439 (92%)	441 (92%)	
Patient						
Yes	89/89 (100%)	25 (28%)	< 0.00001	20/86 (23%)	20/89 (22%)	0.90
No		64 (72%)		66/86 (77%)	69/89 (78%)	

Values are presented as number (percentage)

[#] *p* values are derived from Fisher's exact test

**p* values are derived from McNemar's test

[a] Including a total of 477 nodules from 86/89 positive patients due to degradation from breathing artifacts in 3 patients

arbitrary cutoff for size or number of nodules. Our study results show significantly low sensitivity for lung nodule detection on PET/MR. Nodule size is the most relevant factor affecting sensitivity. A large number of nodules that were missed on PET/MR demonstrated growth. It might seem paradoxical that failure to detect nodules, even when significant, did not impact clinical decision in the setting of primary abdominal malignancies.

The overall sensitivity for detection of lung nodules on PET/MR was 28.1%. Our results are at the lower end of the spectrum compared to other studies (sensitivity 30–83%) [18–24, 32]. The primary reason for this difference is we did not set arbitrary size cut-offs for assigning significance to nodules. Size cut-offs are valid only for incidental lung nodules and not applicable for oncologic patients [33, 34]. In oncology workup, nodules of any size can be significant. In

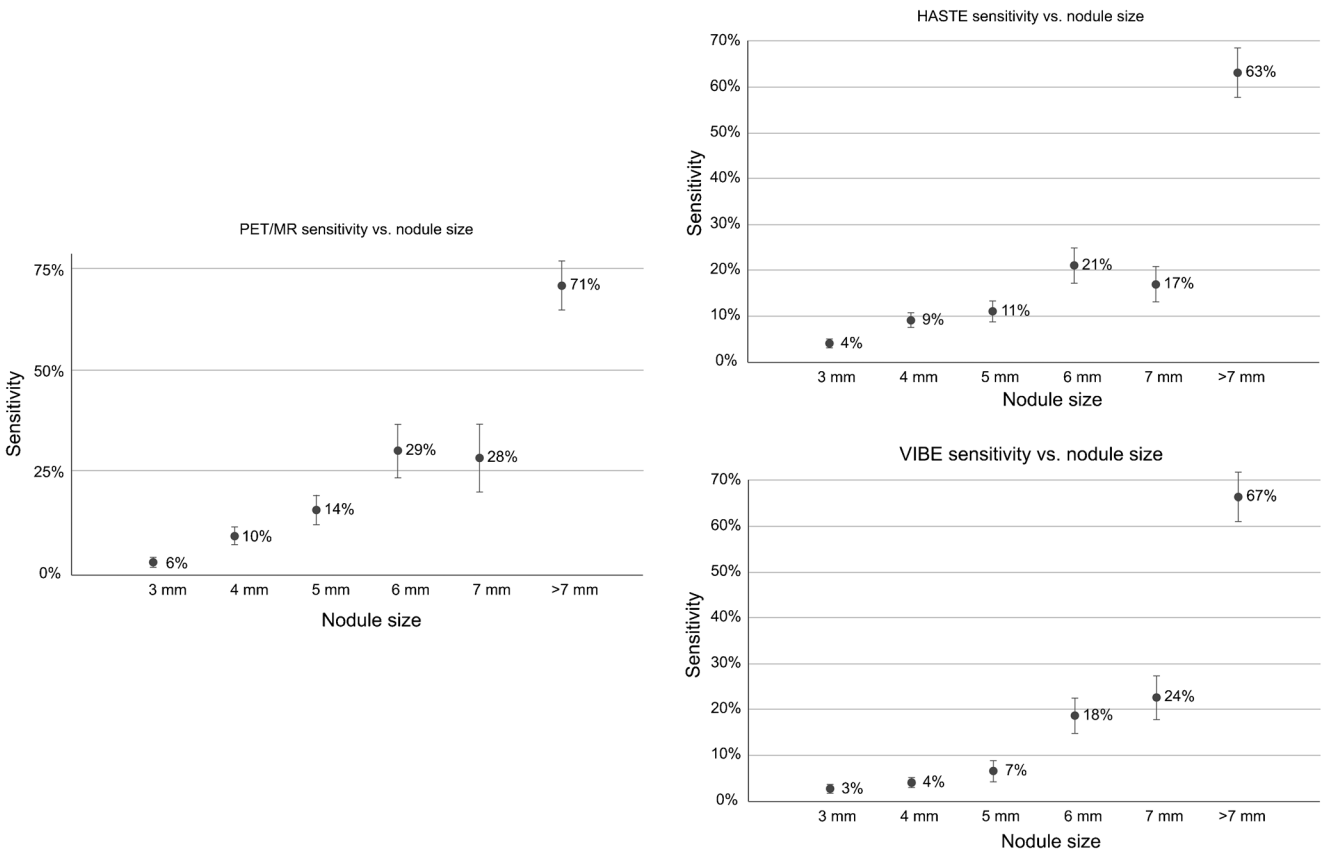

Fig. 2 PET/MR, HASTE, and VIBE plot sensitivity values in detecting lung nodules, based on their size, when compared to standard of care chest imaging (SCI, either PET/CT or chest CT)

Table 6 PET/MR, HASTE, and CE-VIBE sensitivity values in detecting lung nodules, based on size, when compared to standard of care imaging (SCI, either PET/CT or chest CT)

Nodule size (mm)	PET/MRI sensitivity (mean ± SE)	HASTE sensitivity (mean ± SE)	VIBE sensitivity (Mean ± SE)
3	6.5% ± 1.9%	3.9% ± 1.5%	3.2% ± 1.4%
4	10.0% ± 2.8%	9.2% ± 2.6%	3.4% ± 1.6%
5	13.8% ± 4.1%	11.1% ± 3.7%	6.9% ± 3%
6	29.2% ± 9.3%	20.8% ± 8.2%	16.6% ± 7.6%
7	27.7% ± 10.5%	16.6% ± 8.8%	22.2% ± 9.8%
8	70.8% ± 9.3%	62.5% ± 9.8%	66.6% ± 9.6%

SE, standard error

the follow-up of nodules missed on PET/MR, those that increased in size had a mean diameter of 3.8 mm and justifies our reasoning to include all size nodules. For nodules, > 7 mm sensitivity was > 70% which is consistent with other studies [22]. Moreover, we documented all nodules, unlike other literature that set a limit of nodules counted for each patient. In reality, it is difficult to predict the nodules that become significant; therefore, all nodules are deemed important. Furthermore, our reference of standard was diagnostic chest CT and not non-diagnostic attenuation-correction CT as in other manuscripts [21, 24, 35, 36].

The number of sequences that can be used during PET/MR is limited due to time constraints. For abdominal malignancy, the focus is on abdominal viscera and nodes, and more dedicated sequences are prioritized in the abdomen. In this study, we used commercially available, standard of care PET/MR sequences, like inspiratory breath-hold axial T2-weighted HASTE and contrast-enhanced axial and coronal T1-weighted VIBE for the chest, that are part of our routine oncological WB staging protocol. The usage of two different sequences in our study increased nodule detection and provided a synergistic effect. The newer specialized sequences such as UTE and free-breathing STAR VIBE might be advantageous in some instances [37].

The slice thickness of 3 mm for VIBE and 6 mm for HASTE might have played a role in decreasing sensitivity for smaller nodules. At the same time, thinner acquisitions are more likely to result in low-quality images and can have limited utility due to low signal and contrast-to-noise ratios and longer acquisition times. We believe that shorter scan time with breath-holds results in superior image quality and this is supported by similar sensitivity for nodule detection in upper and lower lobes and in central and peripheral nodules.

There was no significant difference in determining [18F]-FDG uptake of nodules when compared to PET/CT. The percentage of [18F]-FDG avid nodules in our population is lower than by other authors, likely due to overall smaller nodule size in our study, probably below PET resolution capabilities [33].

The criteria to determine significance of nodules missed on PET/MR are similar to Chandarana's who relied on ≥ 2-mm growth during follow-up [22]. Unlike other studies [19, 22, 23] with low incidence of significant missed nodules, our study had more significant missed nodules. 22.3% of missed nodules increased ≥ 2 mm, which is a matter of concern and highlights a potentially clinically relevant limitation of current PET/MR staging.

It might seem paradoxical that none of the significant missed nodules affected patient management; similar results were also seen by Raad et al. [23]. However, this is likely explained by the fact that 110/126 patients were already diagnosed with stage III or IV disease and missing lung nodules did not change treatments, including chemotherapy regimens or debulking surgeries. On the other hand, 16 patients with potentially resectable disease were offered the chance to undergo surgery since the sub-centimeter lung nodules were considerete indeterminate at SCI. Therefore, while the management implications of missing lung nodules in our study might be applicable to similar patient populations with extrathoracic advanced stage at PET/MR imaging, they might not be applicable to different populations with less advanced disease at presentation.

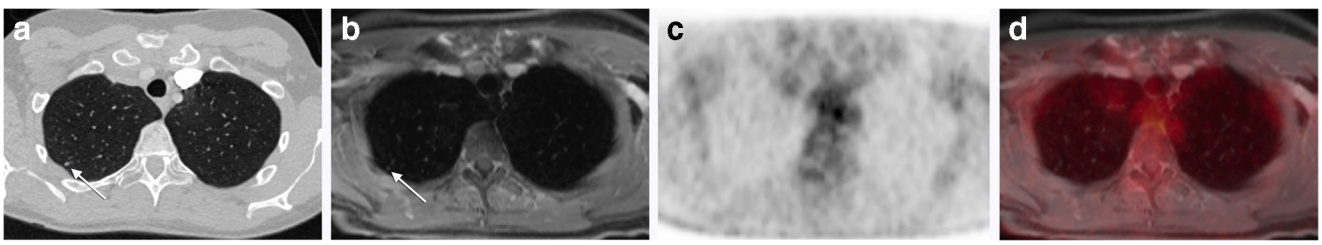

Fig. 3 54-year-old man. Axial stand-alone chest CT (A). PET/MR: corresponding level axial contrast-enhanced VIBE (B), corresponding axial PET (C), and fused PET/MR image (D). A 6-mm nodule in the right upper lobe (arrows) is identified in both A and B. The nodule does not demonstrate [18F]-FDG uptake

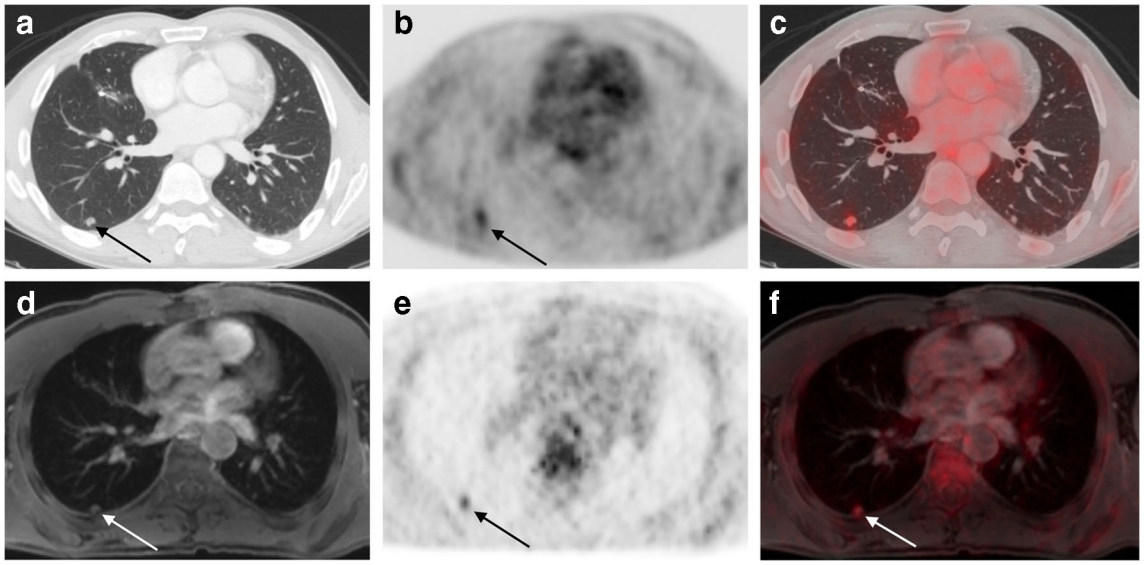

Fig. 4 47-year-old man. PETCT: axial diagnostic quality chest CT (**a**), same level axial PET (**b**), corresponding fused axial PET/CT image (**c**). PET/MR: axial contrast-enhanced VIBE (**d**), same level axial PET (**e**), and corresponding fused PET/MRI image (**f**). A [18F]-FDG avid 11-mm nodule in the right lower lobe (arrows) is seen both on PET/CT and PET/MR

The 6-week time frame between PET/MR and SCI, instead of same-day acquisition of both SCI and PET/MR, represents a limitation in our study. However, the optimal time for cancer-related follow-up has been a subject of debate and indeed relates to the aggressiveness and doubling time of the underlying tumor histology. In lung cancer follow-up, the international guidelines for follow-up range from every 3 months in the first 2 years to 6 months in the first 2 years [38–41]. The most aggressive guidelines by the UK National Institute for Health and Clinical Excellence (NICE) recommends initial follow-up within 6 weeks [42]. Similar guidelines are echoed for abdominal malignancies. The optimal follow-up rate for lung metastases has been studied for colorectal cancers, in which a short-term follow-up of 5–6 months was recommended, based upon a mean tumor volume doubling time of 160 days [43]. The National Comprehensive Cancer Network practice guidelines and the Society of Gynecology Oncology guidelines for vulvar cancer, cervical cancer, ovarian cancer, and uterine cancers also have recommendations of surveillance between 3 and 6 months [44–47]. In this context, there is a paucity of evidence supporting the use of regular CT chest surveillance for metastatic lung nodules, given the relative low yield of finding metastases. Therefore, in face of current literature on oncologic surveillance, we believe that a time interval of 6 weeks is relatively conservative and unlikely to introduce significant bias.

The study is limited by retrospective design and inclusion only of primary abdominal malignancies. Therefore, our findings may not be applicable to other malignancies, where missed metastatic lung nodules can impact management. Moreover, even in the settings of primary abdominal malignancies, difference in organ of origin and even in histology in the case of tumors arising from the same organ, for example, primary pancreatic adenocarcinomas versus primary pancreatic well- or moderately differentiated neuroendocrine cancers, strongly impact on the clinical implications of lung nodules/metastases. In this respect, our study suffers from the intrinsic limitations of having recruited a heterogenous population in terms of organ of origin, histology, stage, and treatment status. We chose standard MR sequences that can be smoothly incorporated into WB-PET/MR instead of dedicated sequences that might increase lung nodule detection sensitivity but disrupt workflow. It is also possible that missed nodules could affect management in few cases.

In conclusion, PET/MR sensitivity for lung nodule detection was significantly lower than standard of care chest imaging and influenced by size, with improved performance for nodules > 7 mm. The fact that 22.3% of missed nodules grew at follow-up, likely representing metastases, is an important red flag. This should alert about the need of performing a diagnostic quality chest CT to detect lung nodules in patients whose oncologic whole/body staging PET/MR was negative for both extra-thoracic metastases and for lung nodules, especially if detection of lung metastases might change management.

Data availability Data of this study are available upon a reasonable request from the corresponding author, Onofrio Catalano. They are not publicly available due to privacy restrictions.

Compliance with ethical standards

Conflict of interest The authors declare that they have no conflict of interest.

Ethical approval This study was approved by the Human Research Committee of our Institutional Review Board and is compliant with the Health Insurance Portability and Accountability Act.

Consent to participate Written informed consent was waived by the Institutional Review Board due to the retrospective nature of the study.

Consent for publication Not applicable

Code availability Not applicable

References

1. Gould MK, Tang T, Liu I-LA, Lee J, Zheng C, Danforth KN, et al. Recent trends in the identification of incidental pulmonary nodules. Am J Respir Crit Care Med. 2015;192:1208–14.
2. Edge S, Byrd DR, Compton CC, Fritz AG, Greene FL, Trotti A. AJCC Cancer Staging Handbook: From the AJCC Cancer Staging Manual. Berlin: Springer; 2011.
3. Rubin GD. Lung nodule and cancer detection in computed tomography screening. J Thorac Imaging. 2015;30:130–8.
4. Cronin P, Dwamena BA, Kelly AM, Carlos RC. Solitary pulmonary nodules: meta-analytic comparison of cross-sectional imaging modalities for diagnosis of malignancy. Radiology. 2008;246:772–82.
5. Ruilong Z, Daohai X, Li G, Xiaohong W, Chunjie W, Lei T. Diagnostic value of 18F-FDG-PET/CT for the evaluation of solitary pulmonary nodules: a systematic review and meta-analysis. Nucl Med Commun. 2017;38:67–75.
6. Czernin J, Allen-Auerbach M, Schelbert HR. Improvements in cancer staging with PET/CT: literature-based evidence as of September 2006. J Nucl Med. 2007;48(Suppl 1):78S–88S.
7. Poeppel TD, Krause BJ, Heusner TA, Boy C, Bockisch A, Antoch G. PET/CT for the staging and follow-up of patients with malignancies. Eur J Radiol. 2009;70:382–92.
8. von Schulthess GK, Steinert HC, Hany TF. Integrated PET/CT: current applications and future directions. Radiology. 2006;238:405–22.
9. Spick C, Herrmann K, Czernin J. 18F-FDG PET/CT and PET/MRI perform equally well in cancer: evidence from studies on more than 2,300 patients. J Nucl Med. 2016;57:420–30.
10. Rausch I, Quick HH, Cal-Gonzalez J, Sattler B, Boellaard R, Beyer T. Technical and instrumentational foundations of PET/MRI. Eur J Radiol. 2017;94:A3–13.
11. Amorim BJ, Hong TS, Blaszkowsky LS, Ferrone CR, Berger DL, Bordeianou LG, et al. Clinical impact of PET/MR in treated colorectal cancer patients. Eur J Nucl Med Mol Imaging. 2019;46:2260–9.
12. Catalano OA, Rosen BR, Sahani DV, Hahn PF, Guimaraes AR, Vangel MG, et al. Clinical impact of PET/MR imaging in patients with cancer undergoing same-day PET/CT: initial experience in 134 patients–a hypothesis-generating exploratory study. Radiology. 2013;269:857–69.
13. Catalano OA, Daye D, Signore A, Iannace C, Vangel M, Luongo A, et al. Staging performance of whole-body DWI, PET/CT and PET/MRI in invasive ductal carcinoma of the breast. Int J Oncol. 2017;51:281–8.
14. Ferrone C, Goyal L, Qadan M, Gervais D, Sahani DV, Zhu AX, et al. Management implications of fluorodeoxyglucose positron emission tomography/magnetic resonance in untreated intrahepatic cholangiocarcinoma. Eur J Nucl Med Mol Imaging. 2020;47:1871–84.
15. Catalano OA, Nicolai E, Rosen BR, Luongo A, Catalano M, Iannace C, et al. Comparison of CE-FDG-PET/CT with CE-FDG-PET/MR in the evaluation of osseous metastases in breast cancer patients. Br J Cancer. 2015;112:1452–60.
16. Lauenstein TC, Goehde SC, Herborn CU, Goyen M, Oberhoff C, Debatin JF, et al. Whole-body MR imaging: evaluation of patients for metastases. Radiology. 2004;233:139–48.
17. Sieren JC, Ohno Y, Koyama H, Sugimura K, McLennan G. Recent technological and application developments in computed tomography and magnetic resonance imaging for improved pulmonary nodule detection and lung cancer staging. J Magn Reson Imaging. 2010;32:1353–69.
18. Burris NS, Johnson KM, Larson PEZ, Hope MD, Nagle SK, Behr SC, et al. Detection of small pulmonary nodules with ultrashort echo time sequences in oncology patients by using a PET/MR system. Radiology. 2016;278:239–46.
19. Sawicki LM, Grueneisen J, Buchbender C, Schaarschmidt BM, Gomez B, Ruhlmann V, et al. Comparative performance of ^{18}F-FDG PET/MRI and ^{18}F-FDG PET/CT in detection and characterization of pulmonary lesions in 121 oncologic patients. J Nucl Med. 2016;57:582–6.
20. Schwenzer NF, Seith F, Gatidis S, Brendle C, Schmidt H, Pfannenberg CA, et al. Diagnosing lung nodules on oncologic MR/PET imaging: comparison of fast T1-weighted sequences and influence of image acquisition in inspiration and expiration breath-hold. Korean J Radiol. 2016;17:684–94.
21. Rauscher I, Eiber M, Fürst S, Souvatzoglou M, Nekolla SG, Ziegler SI, et al. PET/MR imaging in the detection and characterization of pulmonary lesions: technical and diagnostic evaluation in comparison to PET/CT. J Nucl Med. 2014;55:724–9.
22. Chandarana H, Heacock L, Rakheja R, DeMello LR, Bonavita J, Block TK, et al. Pulmonary nodules in patients with primary malignancy: comparison of hybrid PET/MR and PET/CT imaging. Radiology. 2013;268:874–81.
23. Raad RA, Friedman KP, Heacock L, Ponzo F, Melsaether A, Chandarana H. Outcome of small lung nodules missed on hybrid PET/MRI in patients with primary malignancy. J Magn Reson Imaging. 2016;43:504–11.
24. Stolzmann P, Veit-Haibach P, Chuck N, Rossi C, Frauenfelder T, Alkadhi H, et al. Detection rate, location, and size of pulmonary nodules in trimodality PET/CT-MR: comparison of low-dose CT and Dixon-based MR imaging. Investig Radiol. 2013;48:241–6.
25. Lee KH, Park CM, Lee SM, Lee JM, Cho JY, Paeng JC, et al. Pulmonary nodule detection in patients with a primary malignancy using hybrid PET/MRI: is there value in adding contrast-enhanced MR imaging? PLoS One. 2015;10:e0129660.
26. Bankier AA, MacMahon H, Goo JM, Rubin GD, Schaefer-Prokop CM, Naidich DP. Recommendations for measuring pulmonary nodules at CT: a statement from the Fleischner Society. Radiology. 2017;285:584–600.
27. Revel M-P, Bissery A, Bienvenu M, Aycard L, Lefort C, Frija G. Are two-dimensional CT measurements of small noncalcified pulmonary nodules reliable? Radiology. 2004;231:453–8.
28. Kobayashi Y, Sakao Y, Deshpande GA, Fukui T, Mizuno T, Kuroda H, et al. The association between baseline clinical-radiological characteristics and growth of pulmonary nodules with ground-glass opacity. Lung Cancer. 2014;83:61–6.
29. Lee SW, Leem C-S, Kim TJ, Lee KW, Chung J-H, Jheon S, et al. The long-term course of ground-glass opacities detected on thin-section computed tomography. Respir Med. 2013;107:904–10.
30. Matsuguma H, Mori K, Nakahara R, Suzuki H, Kasai T, Kamiyama Y, et al. Characteristics of subsolid pulmonary nodules showing growth during follow-up with CT scanning. Chest. 2013;143:436–43.
31. Callister MEJ, Baldwin DR, Akram AR, Barnard S, Cane P, Draffan J, et al. British Thoracic Society guidelines for the

investigation and management of pulmonary nodules. Thorax. 2015;70 Suppl 2:ii1–54.
32. de Galiza Barbosa F, Geismar JH, Delso G, Messerli M, Huellner M, Stolzmann P, et al. Pulmonary nodule detection in oncological patients - value of respiratory-triggered, periodically rotated overlapping parallel T2-weighted imaging evaluated with PET/CT-MR. Eur J Radiol. 2018;98:165–70.
33. Bueno J, Landeras L, Chung JH. Updated Fleischner society guidelines for managing incidental pulmonary nodules: common questions and challenging scenarios. Radiographics. 2018;38:1337–50.
34. MacMahon H, Naidich DP, Goo JM, Lee KS, Leung ANC, Mayo JR, et al. Guidelines for management of incidental pulmonary nodules detected on CT images: from the Fleischner Society 2017. Radiology. 2017;284:228–43.
35. Boada FE, Koesters T, Block KT, Chandarana H. Improved detection of small pulmonary nodules through simultaneous MR/PET imaging. Magn Reson Imaging Clin N Am. 2017;25:273–9.
36. Rakheja R, DeMello L, Chandarana H, Glielmi C, Geppert C, Faul D, et al. Comparison of the accuracy of PET/CT and PET/MRI spatial registration of multiple metastatic lesions. AJR Am J Roentgenol. 2013;201:1120–3.
37. Frenk NE, Montesi SB, Chen T, Liang LL, Zhou I, Seethamraju R, et al. Free-breathing dynamic contrast-enhanced magnetic resonance of interstitial lung fibrosis. Magn Reson Imaging. 2020;69:16–21.
38. Saunders M, Sculier JP, Ball D, Capello M, Furuse K, Goldstraw P, et al. Consensus: the follow-up of the treated patient. Lung Cancer. 2003;42(Suppl 1):S17–9.
39. Ettinger DS, Wood DE, Aisner DL, Akerley W, Bauman J, Chirieac LR, et al. Non-small cell lung cancer, version 5.2017, NCCN clinical practice guidelines in oncology. J Natl Compr Cancer Netw. 2017;15:504–35.
40. Colt HG, Murgu SD, Korst RJ, Slatore CG, Unger M, Quadrelli S. Follow-up and surveillance of the patient with lung cancer after curative-intent therapy: diagnosis and management of lung cancer, 3rd ed: American College of Chest Physicians evidence-based clinical practice guidelines. Chest. 2013;143:e437S–54S.
41. Crinò L, Weder W, van Meerbeeck J, Felip E, ESMO Guidelines Working Group. Early stage and locally advanced (non-metastatic) non-small-cell lung cancer: ESMO Clinical Practice Guidelines for diagnosis, treatment and follow-up. Ann Oncol. 2010;21 Suppl 5:v103–15.
42. National Collaborating Centre for Cancer (UK). The diagnosis and treatment of lung cancer (update). Cardiff (UK): National Collaborating Centre for Cancer (UK); 2012.
43. Kim EY, Lee J-I, Sung YM, Cho SH, Shin DB, Kim YS, et al. Pulmonary metastases from colorectal cancer: imaging findings and growth rates at follow-up CT. Clin Imaging. 2012;36:14–8.
44. Koh W-J, Greer BE, Abu-Rustum NR, Campos SM, Cho KR, Chon HS, et al. Vulvar cancer, version 1.2017, NCCN clinical practice guidelines in oncology. J Natl Compr Cancer Netw. 2017;15:92–120.
45. Armstrong DK, Alvarez RD, Bakkum-Gamez JN, Barroilhet L, Behbakht K, Berchuck A, et al. NCCN guidelines insights: ovarian cancer, version 1.2019. J Natl Compr Cancer Netw. 2019;17:896–909.
46. Koh W-J, Abu-Rustum NR, Bean S, Bradley K, Campos SM, Cho KR, et al. Cervical cancer, version 3.2019, NCCN clinical practice guidelines in oncology. J Natl Compr Cancer Netw. 2019;17:64–84.
47. Koh W-J, Abu-Rustum NR, Bean S, Bradley K, Campos SM, Cho KR, et al. Uterine neoplasms, version 1.2018, NCCN clinical practice guidelines in oncology. J Natl Compr Cancer Netw. 2018;16:170–99.